OPTICAL OBSERVATIONS FOR ENERGETIC CHARACTERIZATION OF IN-ORBIT EXPLOSION: THE FREGAT-SB CASE

Gaetano Zarcone[(1)], Lorenzo Mariani[(1)], Matteo Rossetti[(1)], Lorenzo Cimino [(1)], Shariar Hadji Hossein[(1)], Federico Curianò[(2)], Fabrizio Piergentili[(1)], Fabio Santoni[(2)]

(1) Department of Mechanical and Aerospace Engineering (DIMA), University of Rome "La Sapienza"; gaetano.zarcone@uniroma1.it, mariani_lorenzo@hotmail.it, matteorossetti31@gmail.com, lorenzociminho@gmail.com, shariar.hadjihossein@gmail.com, fabrizio.piergentili@uniroma1.it
(2) Department of Astronautics, Electric and Energy Engineering (DIAEE), University of Rome "La Sapienza"; federico.curiano@uniroma1.it, fabio.santoni@uniroma1.it

ABSTRACT

The constant increase of space debris and inactive satellites is the root cause of catastrophic events, such as collisions between a debris and active satellites. One of the events that might generate a large number of debris is the in-orbit explosion. Within this complex framework, it is of paramount importance to use a monitoring and surveillance system to understand the number and the distribution of fragments, in an area around the Earth extremely populated by man-made objects. This entails a growing international interest in Space Surveillance and Tracking (SST), where optical observation stands out as an interesting method to obtain information about orbital objects. In this paper, the Sapienza Space Systems and Space Surveillance Laboratory (S5Lab) presents the results of an observing/observational/observation campaign focused on the energetic characterization of the explosion and the monitoring of the fragments generated by a low orbit explosion of the third stage of the Russian rocket FREGAT-SB (ID 37756).

Keywords: space debris, in orbit explosion, SST, SSA

1 INTRODUCTION

The exponential increase of inactive satellites raises the probability of catastrophic events such as collisions and explosions, which determine the generation of new space debris in orbit. Over the years, this has led to an important increase in the number of uncontrolled objects in space, in a chain reaction which would render spaceflight too hazardous to conduct, as first postulated by Donald Kessler in 1978 [1]. Nowadays there are more space debris in orbit than operational satellites and this poses a problem for the near-Earth environment on a global scale. Since the first serious satellite fragmentation occurred in June 1961 (which instantaneously increased the total Earth satellite population by more than 400%), the issue of space debris within the finite region of space around the Earth has been the subject of growing interest in and concerns over Space Surveillance and Tracking (SST) [2].

In the complex framework of fragmentation, it is important to understand the distribution and the number of space debris for the future of spaceflights itself. This involves the fundamental aspects of observing and monitoring the evolution of the fragments from the first fragmentation moment and understanding their distribution from the principal body, to which they belonged. Another important aspect is to characterize energetically these fragments to understand the severity of the event. In this contest, optical observations are an interesting method to obtain information about orbital objects and hold great promise to provide a cost-effective means to monitor orbital debris [3].

Sapienza Space Systems and Space Surveillance Laboratory (S5lab) research team has several years of experience in optical observations, and systems manufacturing [4-17] and for the first time it had to deal with the in-orbit explosion issue. A strategy of observation and an analysis method have been developed to understand these important aspects. The monitoring method requires a strategy, in particular after the initial fragmentation days, when the distance from the original body is too large and it is not possible to detect the fragments by only tracking the principal body. A strategy is possible under the isotropic explosion hypothesis and from the orbital information released by North American Aerospace Defense Command (NORAD), in Two Line Elements (TLE) format. Once the images are obtained, a preliminary and necessary analysis involves an astrometric resolution and the determination of the objects' coordinates. The second step is to check that the measures are not listed by NORAD, meaning that the previously identified coordinates are not associated to an object catalogued by the American agency. In the end, it is possible to carry out several analyses on the unknown objects, classified as possible fragments.

This paper illustrates the approach to the fragmentation problem and its resolution. Once the initial simplified hypothesis is shown (Section 2), the observation strategy is introduced (Section 3). The astrometry phase (Section 4), useful to retrieve the celestial coordinates of the

fragments, is fundamental in order to check the results of the analysis of the observation strategy (Section 5) and to improve the impulse association in terms of velocity variation (Section 6). Moreover, a procedure to estimate the fragments' magnitude is shown (Section 7). The whole process was applied to the observational campaign of the fragmentation event that regarded the third stage of the Russian rocket FREGAT-SB, exploded on May 8, 2020 (Section 8). The observational campaign took place through the observatory system Sapienza Coupled University Debris Observatory (SCUDO) in Collepardo (FR, Italy), which is part of the S5Lab telescope network [8], using a Charge-Coupled Device (CCD) sensor.

Figure 1. SCUDO observatory, Collepardo (FR, Italy)

2 ISOTROPIC EXPLOSION

One of the main causes of the space debris increase is certainly the breakup of a satellite. This kind of events is supposed to have generated hundreds of thousands of fragments larger than 1 cm [18]. Most of the times, the occurred fragmentation is due to residual fuel in tanks or in fuel pipes remained on board once the satellite is released in orbit around the Earth. As its first direct consequence, the explosion of an object entails the generation of a certain number of fragments smaller than the original body. Each of these fragments undergo an impulse in terms of velocity variation, that is totally random in direction and magnitude, making the study of the problem difficult to generalize and model. However, a hypothesis of first approximation useful to simplify the problem is the theory of the isotropic explosion. Such fragments are supposed to receive a certain impulse ΔV in all directions; it is also assumed that these impulses are all equal in magnitude: some tangential and in agreement with the velocity of the original body, others tangential but in the opposite direction, others radial, others more out of plane.

Under the isotropic explosion hypothesis, three phases can be identified following an explosion: the generation of a pulsating ellipse, the formation of the torus, and the disintegration of the latter. In the first phase, fragments that are affected by a purely tangential impulse are considered: if it is synchronized with the velocity of the initial body, the effect is to raise the fragment's orbit, therefore increasing its semi-major axis and decreasing its speed, while an opposite impulse causes the opposite effect. It is possible to establish a relationship between the variation of both the semi-major axis (Δa) and the eccentricity (Δe), and the variation of speed (Δv) radial and tangential:

$$\Delta a = \frac{2a^2}{h}[e\sin(\nu)\,\Delta V_r + (1 + e\cos(\nu)\Delta V_t)] \quad (1)$$

$$\Delta e = \frac{r}{h}\{[1 + e\cos(\nu)\sin(\nu)]\Delta V_r + \\ +[2\cos(\nu) + e(1 + \cos^2(\nu))]\Delta V_t\} \quad (2)$$

where r is the position, a is the semimajor axis, e the eccentricity, ν the true anomaly, ΔV_r and ΔV_t are the radial and tangential impulse respectively, and h is the angular momentum.

Using the orbital period T, it is possible to calculate the angular velocity variation (Δω) undergone by the fragment as a result of the tangential impulse to which the closing time of the ellipse will be tightly correlated. The second phase leads to the generation of a toroidal structure: before the perturbations give evident effects on the orbit motion, there is a time interval in which all the particles will have to pass through the point of the explosion. It is therefore an irregular torus because it collapses in a point called pinch-point. In the third phase the disintegration of the torus takes place due to the perturbations. The main effects come from: J2 perturbation, the lunar-solar one, and the atmospheric drag (the latter must be considered only within the LEO orbital regime).

Of course, the isotropic model of explosions is a first approximation of what reality is; in fact, each fragment will receive a different impulse from the others with a completely random direction. In general, the variations in the orbital plane of the various fragments are, at least initially, less relevant from the point of view of cloud tracking than the variations in the plane.

3 OBSERVATION STRATEGY

An efficient observation strategy is fundamental in order to detect as many fragments as possible. Different strategies have been proposed over the years, both for asteroids and satellites fragmentation, based on several criteria [19-22].

As previously mentioned, the various impulses generated by the explosion take on different intensities and directions and it is therefore reasonable to think that some of these impulses remain on the orbital plane. Therefore, the S5Lab research team followed a first analysis focused on an observation that covered the whole orbital plane to get a first idea of the behavior of the fragments and their number. To do this, a mean anomaly variation (ΔM) is imposed on the original body TLE obtaining a set of

simulated TLEs which differ from the original one because of mean anomaly. The observation strategy is carried on by using a sidereal tracking, thus the stars appear as dots in the images, whereas the object appears as a tracklet, see Fig. 3B.

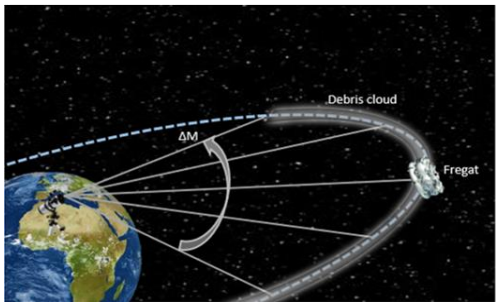

Figure 2. Mean anomaly variation observation strategy

4 ASTROMETRY PHASE: CELESTIAL COORDINATES RECONSTRUCTION AND UNKNOWN DETECTION

Once the images have been acquired, the tracklet is identified in the field of view. Then the celestial coordinates are retrieved resolving the star field using a local version of Astrometry.net with the Tycho-2 star catalogue [23-24]. The process is shown in Fig. 3:

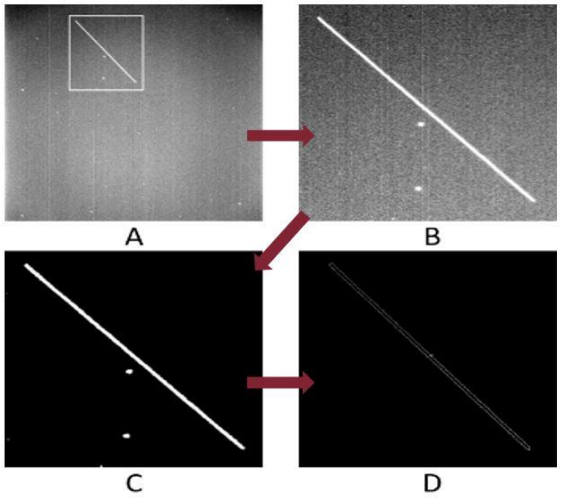

Figure 3. Tracklet detection: bounding box selection (A), filter application (B), threshold (C), tracklet edge detection (D)

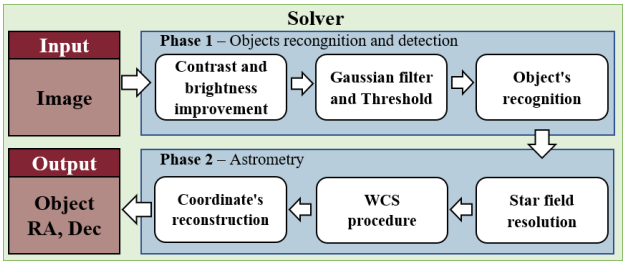

Figure 4. Flow chart of the astrometric analysis software

Knowing the coordinates of the tracklet center, right ascension (Ra) and declination (Dec), allows to understand whether or not the object in the image is already catalogued by NORAD; each TLE in the list published by the American agency is propagated up to the date and time of the measurement, obtaining Ra and Dec. If these celestial coordinates differ from those obtained by the astrometric analysis software by a value less than a certain tolerance, then the object in the image is considered catalogued; otherwise, the object is not present in the catalogue (unknown) and it is therefore likely that the object is a fragment generated by the explosion.

5 ANALYSIS OF THE OBSERVATION STRATEGY RESULTS FOR ENERGETIC CHARACTERIZATION

The subsequent analysis was carried out with the aim of characterizing the explosion in terms of energy. The obtained results do not consider the exact moment in which the explosion occurred, since it is unknown, but the time of release of the last TLE was chosen as such. Furthermore, only semi-major axis and eccentricity were changed, whereas other orbital parameters were deemed constant. Assuming only a tangential impulse, the Eq. 1 and Eq. 2 are simplified since the terms related to the radial impulse are null. To understand the magnitude of the impulse, in terms of tangential ΔV, an iterative procedure was used. It is summarized in Fig.5 which report the flowchart of the process.

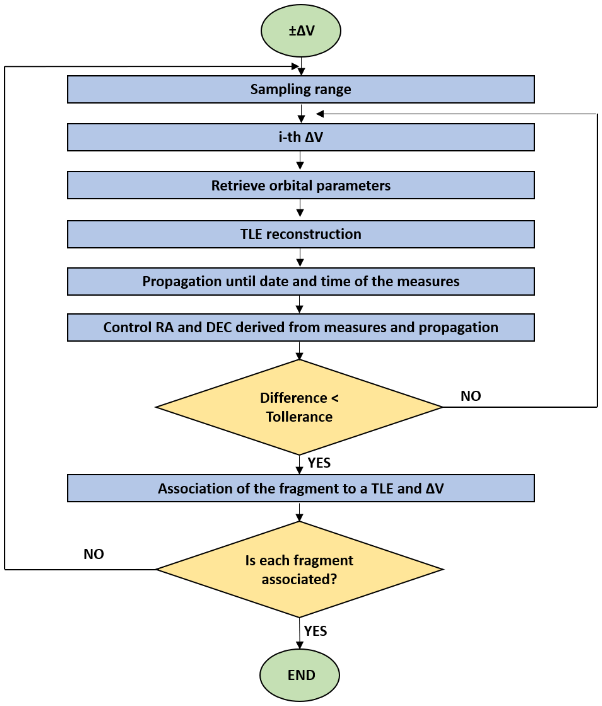

Figure 5. Flowchart for impulse assignment

6 IMPROVEMENT OF THE ΔV ASSOCIATION

To improve the energetic characterization of the ΔV association, a specific analysis was conducted. This analysis is based on comparing the angular distance between the fragments and the original body at the observation date, with the angular trend obtained for a specific imposed impulse. The angular distance between the fragments and the original body can be calculated from the angle between two vectors in the same reference frame. In this case the Earth Centred Inertial (ECI) frame is used. The ECI position of the original body is calculated from the propagation of TLE at the epoch when the fragments have been detected. The position of the fragment obtained from the astrometric procedure is in a topocentric reference frame, thus centered in the observation site. From RA and Dec it is possible to only calculate the unit vector. To calculate the position vector *r* of the fragments in ECI reference system as the sum of the ECI position of station *R* and the topocentric vector ρ, it is necessary to compute the magnitude of vector ρ.

To estimate the magnitude of ρ, the Carnot formula is used:

$$r^2 = R^2 + \rho^2 + 2\rho\vec{R}\hat{L} \tag{3}$$

where $\hat{L}$ is the unit vector of ρ in topocentric frame, whereas the value of r is unknown. In first approximation, it is possible to normalize the value of the magnitude radius *r* as the value of the semi major axis. This approximation is acceptable for low eccentricity orbits.

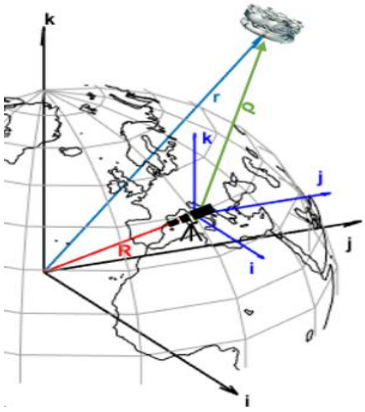

Figure 6. Vector position in the ECI reference frame (black) and topocentric reference frame (blue): the knowledge of the topocentric position ρ of the fragments (green) and of the observatory position R in ECI (red), allows to compute the ECI position r of the fragments (light blue)

In the specific case of the fragments generated by explosion this hypothesis is confirmed since the variation of the shape and dimension after a contained tangential impulse is quite limited. Under this hypothesis, it is possible to calculate the range distance ρ between the observation site and the fragments using Eq. 3. Once the position vector *r* in the ECI frame is obtained, it is possible to estimate the angular distance between the original body and the fragments at the epoch of the observation. A comparison between these angular differences and the angular trend for a characteristic impulse is performed in order to confirm the impulse assignment. To estimate the angular trend, a characteristic impulse to the original body is imposed. The Eq. 1 shows the relation between the semi-major axis variation and the tangential impulse, and vice versa. Therefore, a tangential velocity variation also means a semi-major axis variation, which implies a mean motion variation. This parameter appears in the second line of the TLE, so for each characteristic impulse a new TLE, with modified mean motion, can be obtained. These TLEs are propagated for the whole period of observation campaign and the angular distance from the original body is calculated. Once the angular trends for these particular impulses are obtained, it is possible to assess if a correspondence exists between these trends and the angular distances from the original body, which were found for the fragments.

7 MAGNITUDE ESTIMATION

In order to complete the study, a routine for the magnitude estimation is performed. Initially, the star field resolution is necessary, since it provides a correspondence file that allows to obtain, for each star identified in the Field of View (FoV) the following parameters:

- Ra, Dec star position
- star magnitude from Tycho-2 catalogue
- star intensity
- star background.

The magnitude of each star in the FoV is computed in relation to each of the other stars:

$$\mathrm{mag_i} = \mathrm{mag_{j,cat}} - 2.5\ \log_{10}\frac{\mathrm{I_i}}{\mathrm{I_j}} \tag{4}$$

where mag_i is the magnitude of the i-th star computed with respect to the j-th star selected in Fov. I_i is the intensity associated to the i-th star and it remains constant, whereas $mag_{j,cat}$ and I_j vary according to the j-th star used as reference. Then, a mean value of the i-th star magnitude is computed, associated to an error with respect to the value of the catalogue. Evaluating the results, it is possible to show that to improve the magnitude estimation it is necessary to perform a correct estimation of the stars intensities. To this aim, the so-called Aperture Photometry (AP) procedure [25] is applied. The AP allows to compute the total integrated source signal (S), the background (B) and the objects/star intensity (I) using the Eq. 5:

$$I = S - n_{pix} \cdot B \quad (5)$$

where n_{pix} is the number of pixels within the first circle. The procedure is applied to each star present in FoV. It is possible to notice that the intensity computation strongly depends by the size of the radius which contains the star, see Fig. 7.

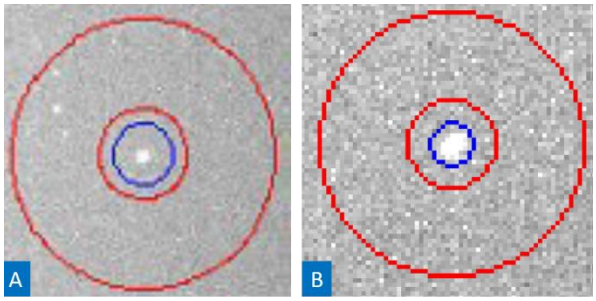

Figure 7. (A) Photometry circles around a star. The blue one contains the star and so the total integrated source signal. The red ones form a circular crown from which is extracted the background. (B) Photometry circles with optimum radius determined

It is demonstrated that exists an optimum value of this radius [25] that maximize the signal to noise ratio (SNR). To find it, an iterative procedure is applied, as in [26]. Once the optimum radius is computed, the next step is to calculate the object magnitude using Eq. 4. It is possible to improve the magnitude calculation using a part of the stars present in FoV which minimize the standard deviation of the error. Therefore, the object magnitude can be computed exploiting Eq. 5 using the object intensity. Applying this procedure to an object and considering a best combination formed by *m* stars, each star intensity is compared with the object intensity, producing *m* values of object magnitude. From these *m* magnitude measures it is computed a mean value. The object intensity is determined in the same way illustrated for the stars, and so through the AP procedure.

8 RESULTS OF REAL CASE TEST: FREGAT-SB

These strategies and analysis methods were validated on the real case of the fragmentation event of the Russian third stage FREGAT-SB (NORAD ID 37756) which occurred on May 8th, 2020 between the 04:00:00 UTC and 06:00:00 UTC. The 3D model of the FREGAT is shown in Fig. 9 and the total number of observations in Fig. 10.

The observations were carried out in the period from May 21st and May 26th, 2020 from SCUDO observatory.

Figure 8. 3D Model of the FREGAT-SB #37756.

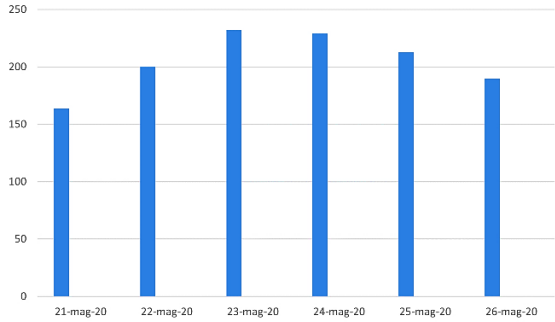

Figure 9. Number of images acquired in the days immediately following the breakup event.

The observation strategy was performed using a mean anomaly variation of 10 degrees, leading to the generation of 36 TLEs. Once the measures have been obtained, the unknown objects found following the procedure in section 3 are reported in Fig. 10. The obtained data made it possible to associate a variation in apogee and perigee altitude with the various fragments related to the orbital period as shown in the Gabbard graph (Fig.11).

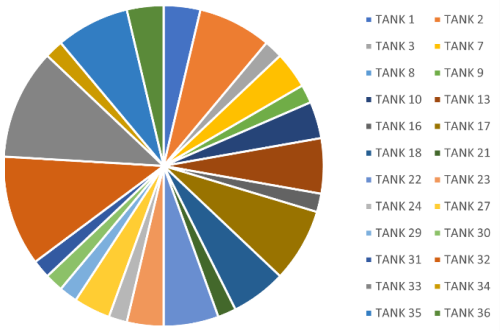

Figure 10. Unknown detected.

These graphs show the results obtained from the measurements acquired in relation to the results obtained by analyzing the TLEs released by NORAD in the months following the explosion. These TLEs were backwards propagated up to the date and time of the measurements. It can be seen how the magnitude of the

impulse, either positive or negative, is responsible respectively for a rise of the apogee or a lowering of the perigee level. The green boxes in the Gabbard diagram highlight the areas of the apogee and perigee values for the present case and it can be observed that with the values of impulse range set at the beginning, the perigee altitude has remained almost constant.

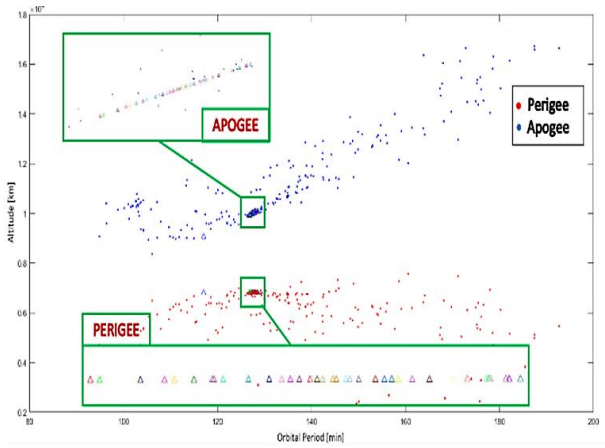

Figure 11 Gabbard diagram: fragments due to FREGAT explosion (green box) and the fragments TLE released by NORAD (blue and red point)

From the analysis of the acquired images, an attempt was therefore made to characterize the explosion of the rocket from an energy point of view, or in any case of a certain number of fragments out of the total generated by the explosion. To demonstrate this, a subsequent analysis was conducted using the TLEs released by NORAD and assigned to different fragments in the months following the event. As for the comparison between the TLEs generated by the previous method and the TLEs released by NORAD, 10 matches were found that differ by a few meters per second in most cases. This would confirm the identification of these fragments. The low values — in the order of tens of meters per second — of maximum impulse obtained in terms of ΔV can be linked to the limitations of the telescope, and probably to the reduced mass of the fragments. The analysis of the angular distance with respect to the angular trends led to a suitable result: mostly of the impulse assignment have been confirmed by this analysis.

The magnitude estimation procedure starts from the stars' optimal radius computation. With the optical system used, and for the images obtained from the observation campaign, the optimal radius led to a mean error in stars magnitude computation of 0.123. The procedure illustrated in section 7 was applied to each image for each observation day and the magnitude estimation of the fragments led to the results shown in Tab.1.

Table 1. Fragments mean magnitude estimation and mean error.

Date	Mean Magnitude [mag]	Mean Std [mag]
21 May 2020	11.5969	±1.2447
22 May 2020	11.7403	±1.3833
23 May 2020	10.5934	±1.9929
24 May 2020	9.1206	±1.1027
25 May 2020	11.0104	±0.9487
26 May 2020	11.9015	±1.5345

All the fragments detected have a mean value of the magnitude equal to 10.99, while the high value of standard deviation could depend on the material of the observed fragment or by its attitude motion which is unknown and affects the sunlight reflectivity toward the observer. Moreover, the mean value of the magnitude is in accord with the report presented by the European Space Surveillance and Tracking (EUSST) [27] which estimate the magnitude in a range of values between 10 and 12.

9 CONCLUSION

In this work, a strategy to analyze an in-orbit explosion was presented. The observation campaign was carried out during the month of May from the SCUDO observatory, based in Collepardo (FR), Italy, and managed by the S5Lab research team. The target was the third stage of the Russian rocket FREGAT-SB (NORAD ID 37756, Int. Deign. 2011-037B) exploded on May 8th ,2020 between the 04:00:00 UTC and 06:00:00 UTC. Starting from optical images acquisition, through the analyses reported in this paper, an initial energy characterization to the event was given. The isotropic explosion hypothesis has proved a suitable approximation of the real problem so much so that it was seen how this analysis is confirmed by the data released by NORAD. Moreover, the observation strategy turned out to be profitable in terms of fragments detection. In fact, about 30% of the total fragments (65 according to 18 Space Control Squadron (18 SPCS) [28]) have been detected pursuing the strategy described in section 8. The next impulses analysis allowed to associate many of them, in the order of meters per second, to all fragments detected. All measures and impulses association have been checked following the procedure presented in section 6, showing consistent results with the analysis strategy. With regards to the magnitude analysis, the procedure proposed led to good results, since the estimate of the fragments magnitude is very close to the EUSST

one. The high value of the standard deviation could be attributable to the unknown attitude motion behavior of the object that affects the magnitude calculation.

10 ACKNOWLEDGEMENTS

The authors acknowledge the support of the Italian Space Agency through the grant agreement n. 2020-6-HH.0 (Detriti Spaziali – Supporto alle attività IADC e SST 2019-2021).

11 REFERENCES

1. Kessler, Donald J.; Cour-Palais, Burton G. (1978). *"Collision Frequency of Artificial Satellites: The Creation of a Debris Belt"*. Journal of Geophysical Research. 83: 2637–2646.
2. Whitlock, D.O. et al., *History of on-orbit satellite fragmentations*, 13th Edition, 2004.
3. Shell, Jim. (2010). *Optimizing Orbital Debris Monitoring with Optical Telescopes*. 18.
4. Diprima, F. Santoni, F. Piergentili, F. Fortunato, V. Abbattista, C. Amoruso, L. *Efficient and automatic image reduction framework for space debris detection based on GPU technology*, (2018) Acta Astronautica, 145, pp. 332-341
5. Sciré G., Piergentili F., Santoni F., *Spacecraft Recognition in Co-Located Satellites Cluster Through Optical Measures*, (2017) IEEE Transactions on Aerospace and Electronic Systems, 53 (4), DOI: 10.1109/TAES.2017.2671619.
6. Piergentili, F., Santoni, F., Seitzer, P., *Attitude Determination of Orbiting Objects from Light curve Measurements*, (2017) IEEE Transactions on Aerospace and Electronic Systems, 53 (1), pp. 81-90, DOI: 10.1109/TAES.2017.2649240.
7. Cardona T., Seitzer P., Rossi A., Piergentili F., Santoni F., *BVRI photometric observations and light-curve analysis of GEO objects*, (2016) Advances in Space Research, 58 (4), pp. 514-527. DOI: 10.1016/j.asr.2016.05.025.
8. S. Hadji Hossein et al., "*Sapienza Space debris Observatory Network (SSON): A high coverage infrastructure for space debris monitoring*," Journal of Space Safety Engineering, 2019, doi: 10.1016/j.jsse.2019.11.001.
9. F. Santoni F. Piergentili T. Cardona F. Curianò F. Diprima S. Hadji Hossein, C. Canu, L. Mariani, EQUO - *Equatorial Italian Observatory at The Broglio Space Center For Space Debris Monitoring*, IAC-17,A6,IP,10,x38808, 2017.
10. Piergentili F., Ceruti A., Rizzitelli F., Cardona T., Battagliere M.L., Santoni F., *Space debris measurement using joint mid-latitude and equatorial optical observations*, (2014) IEEE Transactions on Aerospace and Electronic Systems, 50 (1), pp. 664-675.
11. Pastore, R., Delfini, A., Micheli, D., Vricella, A., Marchetti, M., Santoni, F., Piergentili, F., *Carbon foam electromagnetic mm-wave absorption in reverberation chamber*, (2019) Carbon, 144, pp. 63-71.
12. J. Piattoni, A. Ceruti, and F. Piergentili, *Automated image analysis for space debris identification and astrometric measurements*, Acta Astronaut., vol. 103, pp. 176–184, Oct. 2014.
13. Micheli, D., Santoni, F., Giusti, A., Delfini, A., Pastore, R., Vricella, A., Albano, M., Arena, L., Piergentili, F., Marchetti, M., *Electromagnetic absorption properties of spacecraft and space debris*, (2017) Acta Astronautica, 133, pp. 128-135.
14. Piergentili, F., Porfilio, M., Graziani, F., *Optical campaign for low earth orbit satellites orbit determination*, (2005) European Space Agency, (Special Publication) ESA SP, (587), pp. 689-692.
15. M. Porfilio, F. Piergentili, and F. Graziani, *Two-site orbit determination: The 2003 GEO observation campaign from Collepardo and Mallorca*, Adv. Space Res., vol. 38, no. 9, pp. 2084–2092, 2006.
16. G. Sciré, F. Santoni, and F. Piergentili, *Analysis of orbit determination for space based optical space surveillance system*, Adv. Space Res., vol. 56, no. 3, pp. 421–428, Aug. 2015.
17. F. Piergentili, R. Ravaglia, and F. Santoni, *Close Approach Analysis in the Geosynchronous Region Using Optical Measurements*, J. Guid. Control Dyn., vol. 37, no. 2, pp. 705–710, 2014.
18. ESA,Available:https://www.esa.int/Safety_Security/Space_Debris/About_space_debris. [Accessed: 20-Jan-2020].
19. Drummond, J.D. *A Test of Comet and Meteor Shower Associations*, Icarus, Vol. 45, pp. 545-553, 1981
20. Southworth, R.B. and Hawkins, G.S. *Statistics of Meteor Streams*, Smithsonian Contributions to Astrophysics, Vol. 7, pp. 261-285, 1963.
21. Jopek, T.J. *Remarks on the Meteor Orbital Similarity D-Criterion*, Icarus, Vol. 106, pp. 603-607, 1993.
22. Dimare, Linda & Cicalò, S. & Rossi, A. & Alessi, Elisa Maria & Valsecchi, G.. (2019). *In-Orbit Fragmentation Characterization and Parent Bodies Identification by Means of Orbital Distances*.
23. Hogg, D. W., Blanton, M., Lang, D., Mierle, K., & Roweis, S., 2008, *Automated Astrometry, Astronomical Data Analysis Software and Systems* XVII, R. W. Argyle, P. S. Bunclark, and J. R. Lewis,

eds., ASP Conference Series 394, 27–34.

24. Høg, E., Fabricius, C., Makarov V. V., Urban, S., Corbin, T., Wycoff, G., Bastian, U., Schwekendiek, P.; Wicenec, A., *The Tycho-2 catalogue of the 2.5 million brightest stars.*

25. Howell, S., 2006. *Handbook of CCD Astronomy*, Cambridge University Press.

26. Fabrizio Piergentili, Gaetano Zarcone, Leonardo Parisi, Lorenzo Mariani, Shariar Hadji Hossein and Fabio Santoni, *LEO Object's Light-Curve Acquisition System and Their Inversion for Attitude Reconstruction*, Aerospace 2021, 8(1), 4; doi:10.3390/aerospace8010004

27. EUSST, https://sst.satcen.europa.eu/portal/Fragmentation, *Fragment analysis report*, 4FG-11037B-20200508-003

28. 18SPCS, *https://www.peterson.spaceforce.mil/About/Fact-Sheets/Display/Article/2356622/18th-space-control-squadron/*, accessed on June, 2020